Science of the Total Environment 842 (2022) 156787

Contents lists available at ScienceDirect

Science of the Total Environment

journal homepage: www.elsevier.com/locate/scitotenv

Linking the formation of varves in a eutrophic temperate lake to meteorological conditions and water column dynamics

Maurycy Żarczyński [a,*], Paul D. Zander [b], Martin Grosjean [b], Wojciech Tylmann [a]

[a] Faculty of Oceanography and Geography, University of Gdansk, Gdansk, Poland
[b] Institute of Geography & Oeschger Centre for Climate Change Research, University of Bern, Bern, Switzerland

HIGHLIGHTS

- Decade-long limnological and modern sedimentation observations are presented.
- High-resolution, sedimentary biogeochemical data are tested as a weather proxies.
- Varved lake sediments track past meteorological and limnological processes.
- Calcite lamination corresponds to rapid temperature changes and windiness.
- Manganese deposition tracks holomixis events and hypolimnion oxygenation.

GRAPHICAL ABSTRACT

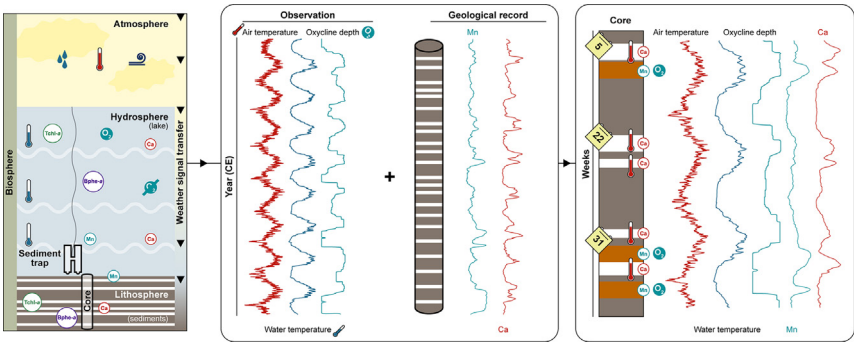

ARTICLE INFO

Editor: Filip M.G.Tack

Keywords:
Varves
Calcite
Manganese
Lake mixing
Paleoweather
Hyperspectral imaging

ABSTRACT

Despite varved sediments being widely used for paleolimnological studies, little information is available about how climate and meteorological signals are recorded in varves at sub-seasonal to annual scale. We investigate links between meteorological and limnological conditions and their influence on biochemical varve formation and preservation of sub-seasonal climate signals in the sediments. Our study site is postglacial Lake Żabińskie located in NE Poland, in which thick and complex varved sediments have been studied for the last decade. These sediments provide an excellent material for studying the influence of short-term weather conditions on geological records. For this, we use an almost decade-long (2012–2019) series of observational data (meteorological conditions, physicochemical water parameters, and modern sedimentation observations) to understand varve formation processes. Then we compare these results with a high-resolution biogeochemical proxy dataset based on μXRF and hyperspectral imaging (HSI) measurements of a varved sediment core spanning the same period. Here we show direct links between the meteorological and limnological conditions and varve formation processes. This is particularly the case for air temperature which governs calcite laminae formation and primary production. We further show that calcite grain size is influenced by lake mixing intensity resulting from the wind activity, and that holomixis events lead to the formation of distinct manganese (Mn) peaks in the typically anoxic sediments. Our findings show that high-resolution non-destructive spectroscopy methods applied to complex biochemical varves, in combination with long observational limnological datasets, provide useful information for tracking meteorological and limnological processes in the past.

1. Introduction

In the face of accelerating human impact on the environment, it is vital to undertake effective conservation and mitigation strategies. These need to be placed into the context of past climate and environmental variability (Neukom et al., 2019). This information can be provided by geological

* Corresponding author at: Division of Geomorphology and Quaternary Geology, Institute of Geography, University of Gdansk, Bażyńskiego 4, PL-80952 Gdansk, Poland.
E-mail address: maurycy.zarczynski@ug.edu.pl (M. Żarczyński).

http://dx.doi.org/10.1016/j.scitotenv.2022.156787
Received 14 April 2022; Received in revised form 14 June 2022; Accepted 14 June 2022
Available online xxxx

records such as lake sediments, which trap information about environmental conditions (Cohen, 2003). However, the attribution of different factors influencing sediment composition and structure is challenging because the atmosphere, hydrosphere, lithosphere, and biosphere form a complex feedback system. This presents a challenge for reliable environmental reconstructions.

Analyses of annually laminated (varved) lake sediments may improve our understanding of these relationships because varve formation is induced by the changing seasonal conditions, which are then reflected in varve structure, providing an opportunity to compare proxy records with instrumental data (Ojala et al., 2012; Zolitschka et al., 2015). For example, clastic and clastic-biogenic varves in high-latitude and high-elevation lakes can accurately register hydroclimate changes, as sediment composition and laminae thickness are influenced by thaw rates, discharge, and erosion intensity and are generally not altered by post-depositional processes (Amann et al., 2017; Francus et al., 2002; Lamoureux, 2000; Ojala et al., 2013). In temperate climate zones, the formation of biochemical varves is often controlled by primary production, epilimnetic temperature, and calcite precipitation (Tylmann et al., 2013; Zolitschka et al., 2015). Here, the climate signal is further modified or lost because of biogeochemical processes taking place in the water column and sediments, as well as human activity, which can lead to a weakening or even loss of the relationship between climate and sediment proxies (Kienel et al., 2013; Poraj-Górska et al., 2017). Thus, finding evidence for mechanistic links between meteorological conditions and sedimentary signals in biochemical varved sediment is challenging and needed.

Revealing information on the climate signal transfer to the sediments is possible by modern process studies bridging monitoring approaches with geological records. This requires high-resolution data from monitoring and sediment cores reflecting seasonal changes within varves. Sedimentation monitoring enables the recognition of primary sediment formation processes, such as seasonal deposition of biotic and abiotic components, and diagenesis (Nuhfer et al., 1993; Scholtysik et al., 2020), while secondary factors such as sediment resuspension can also be traced (Evans, 1994). Additionally, the development of non-destructive scanning methods, such as micro X-ray fluorescence (μXRF) and hyperspectral imaging (HSI), allows for rapid collection of elemental and other biogeochemical data from sediment cores at the micrometer scale (Butz et al., 2015; Croudace et al., 2019).

However, comprehensive studies of short-term relationships between environmental conditions and sedimentation processes in lakes with biochemical varves are rare, as sites offering a long duration of modern sedimentation monitoring and sufficient varve quality are scarce. Biochemical varve sedimentation processes were recently studied via the deployment of sediment traps in Lake Sacrower See (Bluszcz et al., 2008), Lake Suminko (Tylmann et al., 2012), Lake Żabińskie (Bonk et al., 2015a), Lake Kierskie (Apolinarska et al., 2020), Lake Gościąż (Fojutowski et al., 2021), and lakes Tiefer See and Czechowskie (Roeser et al., 2021). The major limitation of these modern sedimentation studies was their relatively short observational periods, making it impossible to catch a range of variability in environmental and meteorological conditions. Thus, how meteorological conditions influence sedimentation and how meteorological signals are recorded in varves is still an open question.

To shed light on the problem outlined above, we investigated Lake Żabińskie in northeast Poland, which offers (i) a decade-long continuous observational data series of meteorological and limnological conditions as well as modern sedimentation as recorded with continuous sediment trap data, and (ii) varves of excellent quality covering the same time interval. Recently, Zander et al. (2021a) used a statistical approach to classify the varves from Lake Żabińskie representing the period 1966–2019 and found characteristic varve types reflecting seasonal variability of some meteorological parameters. In this study, we explore specifically the processes of sediment formation and climate signal preservation in the sediments. We ask the following research questions: 1) Can a reproducible pattern of relationships between meteorological conditions, limnological processes and modern sedimentation be established? 2) Do the surface sediments record the same variability of processes as the sediment traps? 3) What kind of meteorological and limnological phenomena can be precisely tracked with varves? To answer these questions, we compared daily meteorological data with observations of the limnological conditions and sediment trapping carried out between November 2011 and April 2020. Our observational period includes years with substantially contrasting meteorological conditions, encompassing severe winters with prolonged ice-cover and mild winters with largely ice-free conditions and periods of water column mixing and strong thermal stratification. Utilizing the excellent time control based on the varves, we compared these results with the sediment core record spanning the same time frame. High sediment accumulation rates allow biogeochemical data to be obtained at sub-seasonal resolution, and variations in these data could be attributed to varying meteorological and water column conditions. This approach enabled us to identify direct and indirect influences of meteorological conditions and water column dynamics on the sub-seasonal sediment formation in this lake.

2. Study site and methods

2.1. Study site

Lake Żabińskie (54.1318° N, 21.9836° E; 0.42 km^2, 44 m max depth, Fig. 1) is a small, hard water kettle-hole lake located in the Masurian Lakeland, NE Poland. It is situated within the maximum extent of the Pomeranian phase of the Vistulian glaciation, dated to ca. 17–16 ka BP (Marks et al., 2016). Quaternary deposits in the catchment (24.8 km^2) are dominated by glacial tills, sands, and gravels (Szumański, 2000). Lakes Łękuk and Purwin connect to Lake Żabińskie through one inflow, while another inflow (Fig. 1) forming a small delta on the southern bank comes from the nearby village of Żabinka, occasionally bearing high quantities of particulate and dissolved matter (Bonk et al., 2015b). Through an outflow (Fig. 1) on the west, Lake Żabińskie connects with larger Lake Gołdopiwo. The Masurian Lakeland is characterized by pronounced climate continentality. The mean annual temperature of the region is 6.5 °C (Jan. -5.6 °C, Jul. 17 °C), and the annual precipitation sum varies between 550 and 600 mm (Lorenc, 2005). Westerly and south-westerly winds dominate the area (Hutorowicz et al., 1996). Presently, the land cover of the catchment is divided between agriculture and woodlands dominated by oak-lime-hornbeam and pine forests (Wacnik et al., 2016).

Ongoing limnological monitoring indicates that, depending on the meteorological conditions, the Lake Żabińskie mixing regime shifts from meromictic through monomictic to dimictic. Thermal stratification of the water column develops annually, resulting in periods of prolonged anoxia in the hypolimnion. Along with lake depth, basin morphology and high trophy, these conditions favor the formation and preservation of varved sediments (Bonk et al., 2015a).

2.2. Methods

2.2.1. Meteorological data

Daily meteorological data from Kętrzyn (approx. 40 km southwest of the study site) were retrieved from the Institute of Meteorology and Water Management – National Research Institute using open data API and climate 0.9.1 R library (Czernecki et al., 2020). For further analyses, mean daily air temperature at 2 m, mean daily wind speed, and daily precipitation sums were used. Meteorological data are presented in the Supplementary Material (Fig. S1).

2.2.2. Limnological conditions observation

Water parameters, such as temperature, dissolved oxygen concentration (DO), pH, and chlorophyll-*a* concentrations, were measured between November 2011 and April 2020 (Fig. 2). During 2011–2015, a YSI 6820 multiparameter sonde (YSI) was used while chlorophyll-*a* measurements were done using Minitracka IIC fluorometer (Chelsea Instruments). Afterward, an EXO2 multiparameter sonde (YSI) was used. Additionally, a chain of HOBO Water Temperature Pro v2 loggers (ONSET) was installed at the deepest point of the lake. The loggers recorded water temperature at 1, 5,

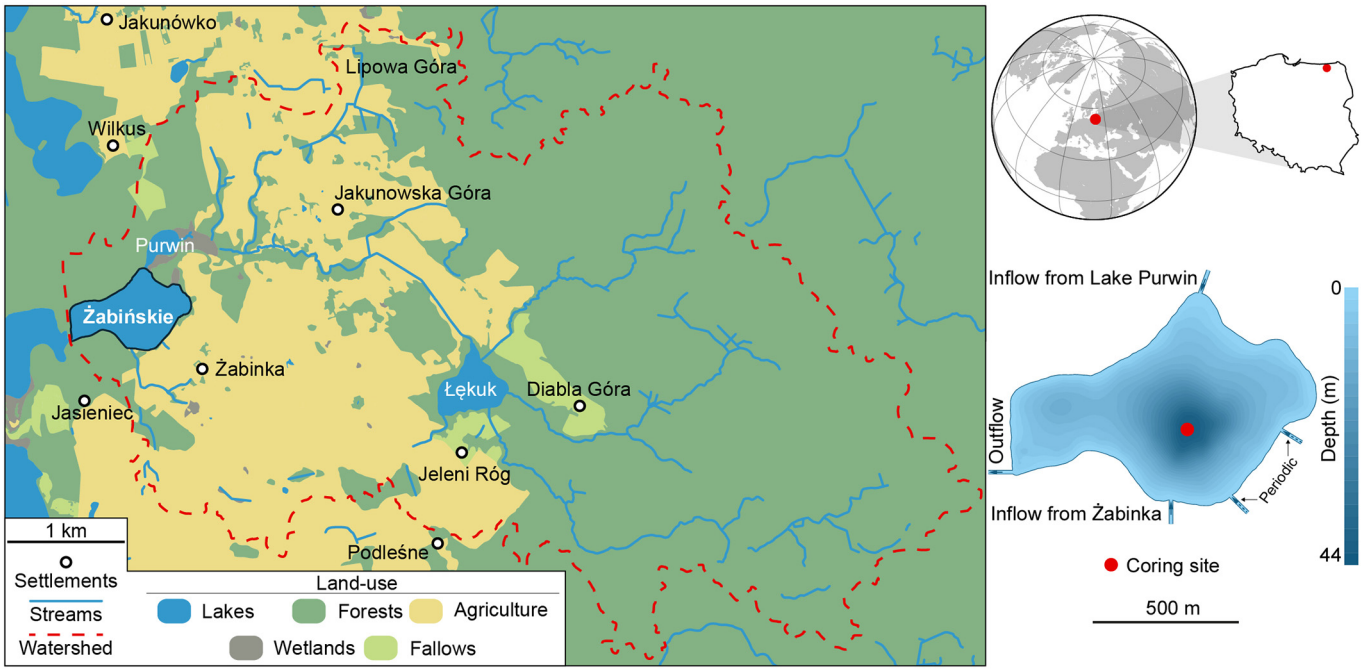

Fig. 1. Site location with bathymetry and coring location. Lake Żabińskie is outlined.

10, 20, 30, and 40 m depth with 15-min intervals. Water transparency was measured with a Secchi disk. Ice-cover dates were established based on field observations and satellite imagery. Water samples from 1 and 40 m depth were used for hydrochemical analyses. Major ion concentrations were determined with ion chromatography (ICS 1100, Dionex). The concentration of bicarbonates was determined with standard HCl titration following Bonk et al. (2015a).

2.2.3. Sedimentation monitoring

Monitoring of modern sedimentation was carried out with a sediment trap made of four 1-m-long PVC liners (ø90 mm; 0.02344 m^2 total active area), located 1 m above the lake bottom at its deepest point (Fig. 3). The sediment trap was retrieved monthly (average interval ≈ 33 days, 69 samples) during the ice-free seasons. Longer periods between trap retrieval occurred during ice-cover (62 to 153 days, seven samples). After collection, samples were freeze-dried and weighed. Mass accumulation rates (MAR; g m^{-2} day^{-1}) were calculated by dividing each sample's mass (g) by the trapping time (days) multiplied by active area (m^2).

2.2.4. Coring and chronology

A 1.33-m-long surface sediment core (ZAB–20/01) was retrieved using a UWITEC gravity corer (ø90 mm) in late April 2020. An undisturbed water-sediment interface was preserved, with the onset of spring calcite accumulation visible. Under laboratory conditions, the core was split lengthwise and photographed. Core half A was subsampled for thin sections, following the procedure proposed by Brauer and Casanova (2001). Ten-centimeter-long slabs were shock frozen with liquid nitrogen, freeze-dried and impregnated with Araldite 2020 (Huntsman) epoxy resin. Slabs were polished at MKfactory (Potsdam, Germany). Detailed microfacies analysis of thin section ZAB–20/01 (0–9.5 cm) was carried out using an Axio Imager A2 microscope (ZEISS) with magnification up to 400×. Due to the short period and excellent varve preservation, repeated varve counts yielded no uncertainty. The thickness of individual calcite layers and the area of calcite grains (μm^2, equivalent to grain size) were measured using ZEN lite software (ZEISS). The thin section was also scanned on a flatbed scanner at 2400 DPI using polarizing foil. Varve coordinates were recorded on scanned images using DotDotGoose 1.5.2 (Ersts, 2020).

2.2.5. Non-destructive scanning

The resin-embedded sediment slab representing the topmost 9.5 cm of the sediment core was used for μXRF measurements using a Tornado M4 μXRF spectrometer (Bruker) at the University of Bern. The scanner was equipped with a Rh tube set to 50 kV and 300 μA. High-resolution 2D maps of elemental compositions were obtained with a 20 μm spot size, 60 μm step size (pixel size), and 20 ms/pixel count time. The fresh core ZAB-20/01 was used for hyperspectral imaging (HSI) with a Specim PFD-CL-65-V10E line-scan camera. The procedure followed Butz et al. (2015) and Zander et al. (2021b), with a spatial resolution of 60 × 60 μm. The abundance of bulk sedimentary pigment groups was determined from their relative absorption band depth (RABD). Calibration to pigment concentrations (μg $g_{d.s}^{-1}$; d.s. = dry sediments) followed Zander et al. (2021b). Total chloropigments-*a* (TChl-*a*), which are used as a proxy of total algal productivity (Butz et al., 2017), are represented by $RABD_{655–685max}$. $RABD_{845}$ represents bacteriopheopigments-*a* (Bphe-*a*) produced by anoxygenic phototrophic sulfur bacteria, a proxy for anoxic conditions in the photic zone (Butz et al., 2016; Sinninghe Damsté and Schouten, 2006). The average reflectance across the spectrum (Rmean) was used as an additional calcite proxy (Butz et al., 2017), corroborating correlation with μXRF data. μXRF and HSI maps are available in the Supplementary Material (Fig. S8).

2.2.6. Elemental analysis

Concentrations of total carbon (TC), total nitrogen (TN), and total sulfur (TS) in the sediment trap samples were determined with a Vario EL Cube elemental analyzer (Elementar). Sediments were freeze-dried, homogenized, and weighted into Sn capsules. For a complimentary analysis of total inorganic carbon (TIC), a SoliTIC module (Elementar) was coupled to the Vario EL Cube. Sediment samples were acidified in the reactor at 50 °C with 5 % HCl to release CO_2. Total organic carbon (TOC) was calculated as the difference between TC and TIC. Precision and accuracy of elemental analyses were tested on certified standard materials B2176 (CNS) and B2188 (TIC) supplied by Elemental Microanalysis. Precision ranges are: TC 0.05 %–1.93 %, TIC 0.04 %–0.45 %, TN 0.01 %–0.22 %, TS 0.01 %–0.05 %.

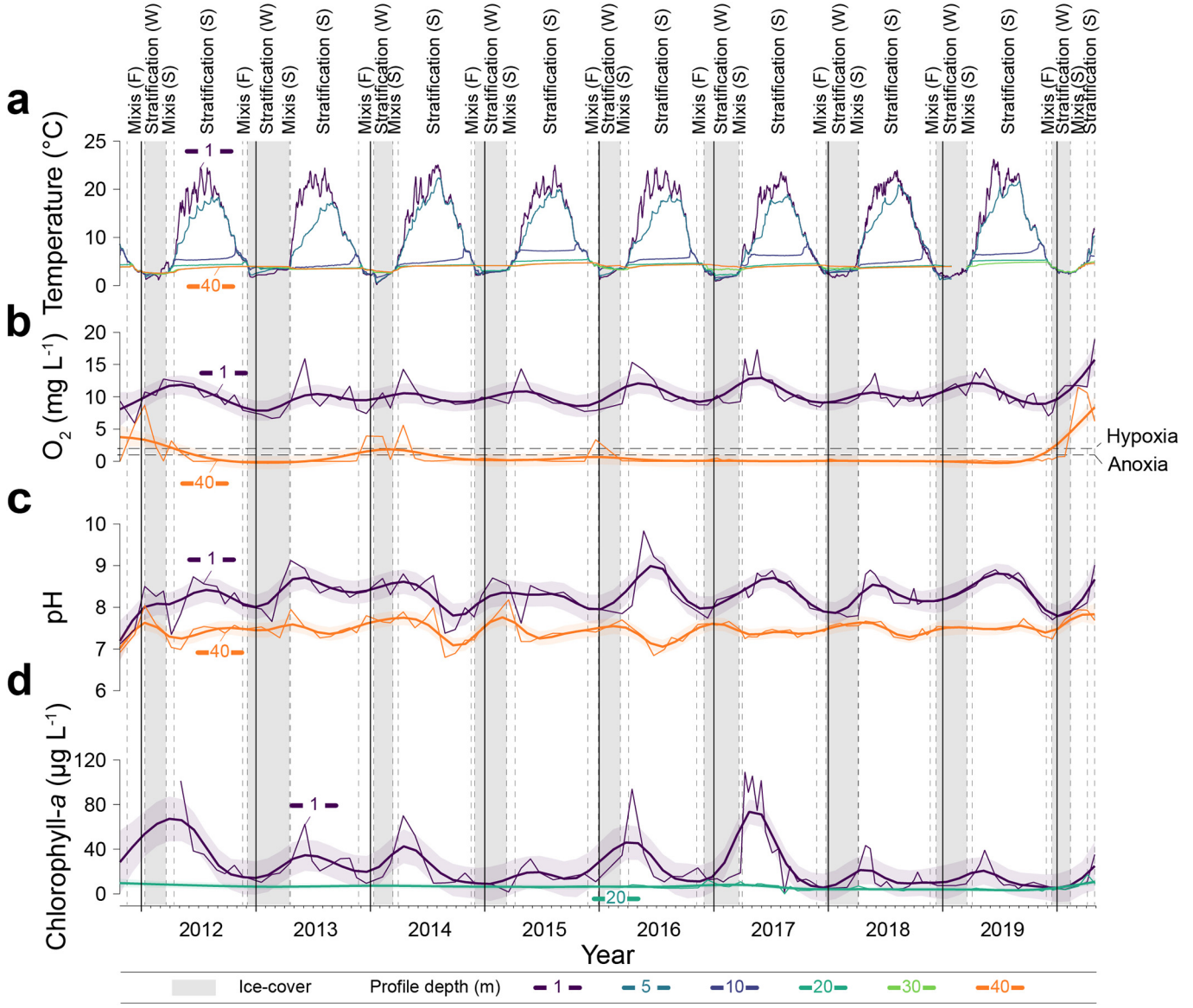

Fig. 2. Time series of selected physicochemical parameters of Lake Żabińskie based on in situ measurements during the years 2011–2020: (a) water temperature; (b) dissolved oxygen concentration; (c) pH; (d) chlorophyll-a concentration. Time series smoothed with generalized additive models (GAMs). Vertical shaded areas mark periods of ice-cover. Periods of mixis or stratification are indicated at the top of the figure.

2.2.7. Powder X-ray diffraction

Powder X-ray diffraction (pXRD) was used for quantitative recognition of selected mineral phases in samples from sediment core and sediment trap material. Sediments were dried, powderized, and then treated with 10 % hydrogen peroxide to remove organic matter. Samples were analyzed at the University of Bern Institute of Geological Sciences using a Panalytical X'Pert PRO MPD equipped with an Empyrean Cu tube. Samples were scanned from 5 to 75° (2θ) with a step size of 0.017° (2θ). Mineral identification was made by comparisons with reference data from the Inorganic Crystal Structure Database using the software TOPAS v6 (Bergerhoff et al., 1987).

2.2.8. Statistics and visualization

All statistical analyses were performed with R 4.1.3 (R Core Team, 2022). Data processing and visualization were carried out with tidyverse 1.3.1 (Wickham et al., 2019) and its components. Physical lake parameters based on the limnological and meteorological monitoring data were calculated with rLakeAnalyzer 1.11.4.1 (Winslow et al., 2019). Schmidt stability was used as a thermal stratification proxy (Idso, 1973). The water column was assumed to be stratified once Schmidt stability exceeded 5 units and the temperature difference between surface (1 m) and bottom (40 m) waters were ≥ 1 °C. Reverse stratification was characterized by periods of a temperature difference between surface (1 m) and bottom (40 m) waters ≤ −1 °C or ice-cover. The remaining days were assumed to reflect homothermic conditions. Principal component analysis (PCA) was used to find relationships between the biogeochemical variables in the core and the main modes of their variation over time. Before multivariate analyses, data were log-transformed, scaled, and centered.

3. Results

3.1. Lake monitoring

The major physicochemical properties of Lake Żabińskie represent a complex stratification regime (Figs. 2, S2). Water temperature changes had a strong, recurrent character (Figs. 2a, S2a). The lake surface was

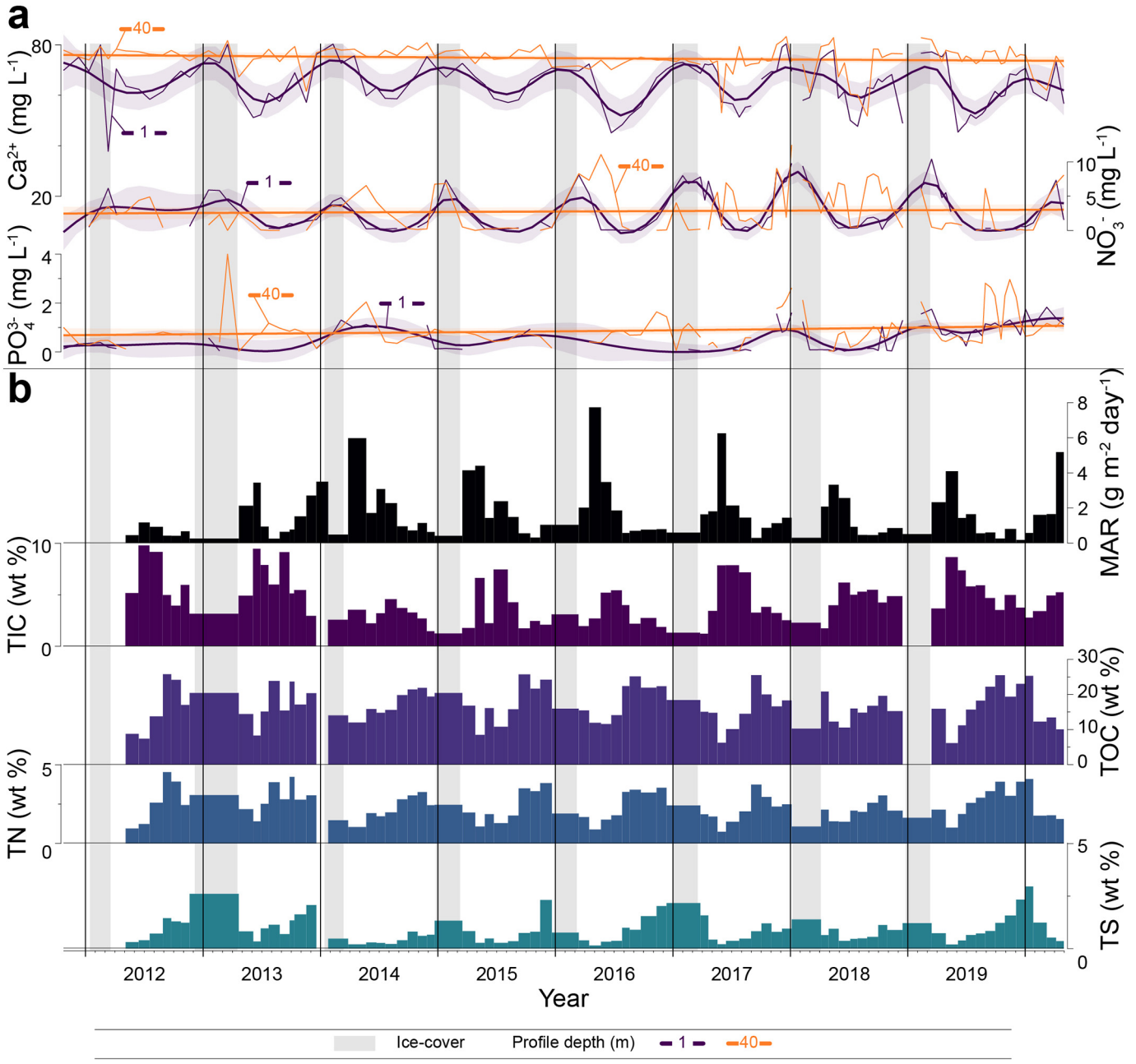

Fig. 3. (a) changes of Ca^{2+}, NO_3^- and PO_4^{3-}; (b) Mass accumulation rate changes and weight % of major sediment components in the sediment trap samples. Vertical shaded areas mark periods of ice-cover.

characterized by the highest temperature variability (10.5 ± 7.6 °C) and the sharpest shifts. Deeper waters were progressively colder, below the depth of 20 m mean values stabilized close to 4.0 °C. Commonly, reverse stratification developed in the winter, especially under the ice-cover. Severe winter conditions led to occasional cooling in the hypolimnion, with temperatures below 3.0 °C. The surface warmed quickly after the yearly ice break-up, with deeper strata following. During summer stratification, the temperature in the epilimnion reached up to 26.2 °C, but at least one profound cooling occurred during every summer (JJA). During the fall, surface waters cooled quickly, whereas temperature at 10 m depth rose abruptly, reaching 8.9 °C. Deeper water layers warmed only briefly.

Dissolved oxygen (DO) concentrations, with the threshold of anoxic conditions set to 1 mg O_2 L^{-1} (Nürnberg, 1995), displayed shifts between oxic and anoxic conditions in the hypolimnion (Figs. 2b, S2b). Typically, oxygen was transported deeper into the water column during the spring turnover after the ice break-up. However, this process was not efficient enough in most years, and the anoxic boundary was established between 20 and 30 m deep. Complete spring oxygenation of the hypolimnion was only registered in 2012 (April, 3.2 mg O_2 L^{-1}), 2014 (April, 5.6 mg O_2 L^{-1}), and 2020 (March, 11.5 mg O_2 L^{-1}). Only the epilimnion remained oxic throughout the summers, with hypoxic conditions developing below around 3 m depth (e.g., June 2013). The fall seasons of 2011, 2013, and 2015 were characterized by complete mixis, when DO concentrations in the hypolimnion reached 5.7, 3.9 and 3.3 mg O_2 L^{-1}, respectively. In other years, the anoxic boundary was established typically between 20 and 30 m water depth. Nonetheless, the fall mixis of 2012 and 2018 did not reach 20 m water depth. Anoxia developed in the bottom waters in winter except during the very warm winter of 2019/20 when fall and spring

turnovers overlapped. Finally, between 2016 and the end of 2019, Lake Żabińskie hypolimnion remained permanently anoxic (meromictic).

Water pH, an important factor controlling precipitation of $CaCO_3$, was highly variable through the monitoring period (Figs. 2c, S2c). Generally, the highest values in surface waters occurred in spring, after the ice break-up and during the phytoplankton blooms. pH tended to decrease in summer, reaching minima before the ice onset. The pH values of the epilimnion occasionally exceeded 10, with a mean value of 8.3 ± 0.4. In the hypolimnion, it was on average lower and steadier (7.5 ± 0.2). In some years, surface and bottom water pH followed similar patterns (e.g., 2013 and 2014), whereas in other years, these two strata exhibited opposite tendencies. The most pronounced difference occurred in 2016.

Chlorophyll-*a* concentrations associated with the phytoplankton abundance varied mostly in the upper 10 m of the water column (Figs. 2d, S2d). Peak concentrations occurred shortly after the ice-cover vanished, reaching the highest values of 220 μg L^{-1} in the spring of 2017. Second, local maxima occurred occasionally during fall. Concentrations below the water depth of 20 m varied only slightly, rarely exceeding 10 μg L^{-1}.

Water temperature, wind speed, and lake morphometry data were used to calculate derivative physical characteristics of Lake Żabińskie's water column. The combination of these results led to the definition of three possible thermic regime phases: 1) summer stratification, 2) reverse (winter) stratification, and 3) mixis periods with a homothermic water column (Fig. 2). Detailed description and visualization of these results are available in the Supplementary Material (Fig. S3). On average, spring mixing lasted for 20 ± 16 days. However, the length of this period varied considerably, reaching up to 27 days (2015 and 2016) when mixing started already in early spring (March). On the other hand, the late (April) onset of mixing led to a substantially shortened period of homothermic conditions (2 days in 2018 and 3 days in 2013). The year 2020 was a clear outlier, with spring mixing starting in mid-February and lasting for 55 days. Fall turnover typically lasted longer (25 ± 15 days). It was the longest in 2011, starting in mid-November and lasting to mid-January (58 days). Additionally, homothermic conditions lasting over 30 days were observed in 2013 and 2015. Contrary to that, the shortest fall mixing took place in 2014 (11 days) and 2017 (14 days).

3.2. Hydrochemistry

Concentrations of Ca^{2+}, NO_3^-, and PO_4^{3-} were used to describe the water column conditions regarding calcite precipitation and availability of nutrients (Fig. 3a). Epilimnetic concentrations of Ca^{2+} (64.38 ± 9.11 mg L^{-1}) showed a recurrent pattern. In general, Ca^{2+} concentrations increased during the reverse stratification and peaked during the mixing events. After the spring turnover, concentrations tended to drop as summer stratification developed. Concentrations in the hypolimnion were less variable and had less pronounced seasonality (74.62 ± 5.26 mg L^{-1}). Nitrate concentrations in the epilimnion showed, on average (2.61 ± 2.81 mg L^{-1}), similar tendencies to Ca^{2+}. The highest concentrations, up to 10.41 mg L^{-1}, were measured in the winter and immediately after the ice break-up. Afterward, during the summer stratification, epilimnetic values reached their annual minima as low as 0.02 mg L^{-1}. Concentrations in the hypolimnion were highly variable (2.81 ± 3.06 mg L^{-1}). Often, maxima in the hypolimnion (up to 12.47 mg L^{-1}) occurred after epilimnion concentrations dropped, and multiple peaks were observed in several years. PO_4^{3-} concentrations in the epilimnion (0.59 ± 0.54 mg L^{-1}) shifted from year to year, with no clear pattern. For example, in 2014, the highest concentrations were associated with summer stratification whereas, during the 2018 summer stratification, the epilimnion was mostly depleted with respect to phosphates. Concentrations in the hypolimnion were typically higher and more variable (0.88 ± 0.71 mg L^{-1}).

3.3. Sedimentation monitoring

Mass accumulation rates and concentrations of major sediment components changed regularly throughout the monitoring period (Fig. 3b). MAR were highest shortly after the spring turnover (May or June), while the lowest MAR were observed during the winter with the lake under ice-cover. Typically, MAR dropped towards the midsummer after the spring peak, whereas another rise was visible near the fall turnover. The average MAR for all samples was 1.60 ± 1.52 g m^{-2} day^{-1} (n = 77). However, throughout the entire monitoring period, MAR varied profoundly from 7.73 g m^{-2} day^{-1} in May 2016 to 0.18 g m^{-2} day^{-1} in December 2019. TOC and TN concentrations, reflecting deposition of organic matter, were closely related to each other throughout the period (r = 0.93, n = 72). TOC and TN concentrations averaged 16.82 ± 5.16 % and 2.37 ± 0.92 %, respectively. The highest concentrations commonly occurred near the end of the summer stratification and during the fall turnover. With the onset of ice-cover, concentrations usually decreased, and the lowest values occurred shortly after the spring mixing. TS, which includes S bound to organic matter and sulfides, was related to the concentrations of TOC (r = 0.60, n = 72, $p < 0.05$) and TN (r = 0.64, n = 72, $p < 0.05$), but its peaks were shifted. Concentrations of TS (mean = 0.88 ± 0.62 %) peaked during winter, frequently exceeding 2.50 %, whereas minima typically occurred in spring and early summer. Deposition of carbonates, represented by TIC (4.40 ± 2.16 %), followed the pattern of MAR changes closely. In most years, TIC concentrations formed a distinct peak shortly after the ice out, reaching up to 9.80 %, whereas the lowest values were observed in the winter, oscillating around 2.50 %. In years with very high sampling resolution (2013, 2015), the spring-summer calcite peak was clearly divided into two parts, whereas in the other years, this could not be observed.

3.4. Sediment core data

3.4.1. Microfacies

Microscopic investigations revealed that all varves represent Type I microfacies, according to Żarczyński et al. (2018). Varve thickness ranged from 4.39 mm to 6.22 mm (sd = 0.53 mm). Each varve year started in the spring with a pale, normally graded calcite lamina mixed with diatom frustules. The size and shape of calcite grains differed significantly among the varve years (Kruskal-Wallis test; df = 8, $p < 0.05$). Spring carbonate layers of 2012, 2014, 2016, and 2020 were composed of larger calcite grains with regular outlines compared to the other years (Figs. 4b, S4, S5). Especially in 2012, 2014, and 2016, calcite crystals were mixed with orange-reddish carbonate grains of rhodochrosite or Mn-rich calcite (Fig. S9). As summer stratification developed, a thin layer of amorphous organic matter mixed with sparse diatom frustules and pyrite formed. A second, typically thinner calcite layer composed of smaller, lighter grains was then deposited. It was typically accompanied by increased diatom abundance, but calcified shells of *Phacotus* algae were also abundant (Fig. S4). Afterward, a mixture of pyrite, organic matter, diatom frustules, and mineral grains (e.g., quartz) were deposited. In 2012, 2015, 2016, and 2017, a third calcite lamina developed (Fig. S6). Sparse vivianite crystals associated with anoxic conditions were visible mostly in 2014. An additional layer comprised of Mn and Fe (oxy)hydroxides formed after intensive fall mixing in 2011 and 2013. Clay minerals mixed with organic detritus were the primary components deposited during reverse stratification under ice-cover. The end of the varve year (early spring) was typically marked by the dominance of diatom frustules (often small, centric specimens) mixed with chrysophyte cysts.

3.4.2. μXRF and HSI

A detailed characterization of element and pigment successions within single varves indicated characteristic, sub-seasonal sedimentation patterns (Fig. 4). Ti and K, commonly used as proxies of mineral matter delivery, showed the highest abundances at the end of each varve year (winter), marking the period when the lake was under ice-cover. The abundances of Fe and S were highest during periods with well-developed summer stratification. Both elements usually reached their respective maxima shortly before peaks of mineral matter. The profile of Mn, an element most often associated with redox changes, was the most intermittent among the analyzed proxies. Clear peaks formed only occasionally, with a visible tendency

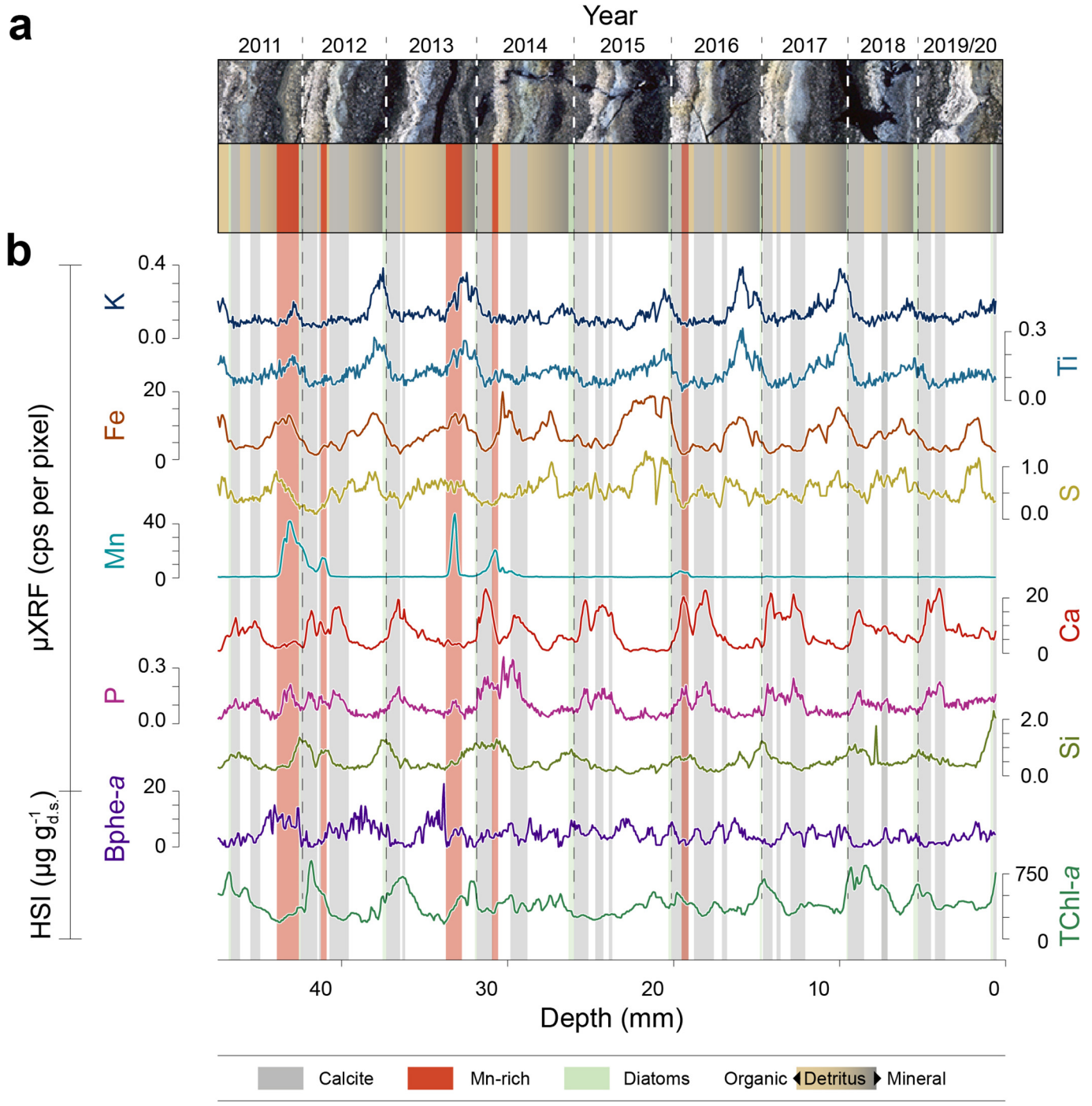

Fig. 4. (a) Thin section scanned in cross-polarized light and microfacies scheme; (b) μXRF and HSI profiles extracted from elemental (resin embedded slab) and pigment (fresh core) maps (data from Zander et al., 2021a).

for two consecutive (fall and spring) peaks, e.g., in 2011/2012 and 2013/2014. Finally, a small increase in Mn abundance occurred at the beginning of 2016. However, this time it was not preceded by higher Mn accumulation in the previous year. Spring peaks of Mn overlapped to some extent with the Ca peaks. Calcium showed a clear annual pattern with sharp increases in spring. In most of the years, Ca maxima were divided into at least two distinct peaks, while in 2013 and 2018, Ca peaks were generally less developed. Abundances of P followed the Ca profile almost exactly. Similar variability is displayed in the profiles of Si and TChl-*a*, with peaks typically in early spring, immediately after the ice-cover disappeared and before Ca peaks formed. Maxima of Bphe-*a* occurred most often in the second half of the year, during the summer stratification. Bphe-*a* peaks were out of phase with carbonates and organic matter proxies, and after 2014, concentrations generally started to drop.

Relationships between the selected proxies were assessed with a PCA (Fig. S7). Ti, K, Fe, S, and Bphe-*a* covaried in a progressing order during the study period. Ca and P formed a second, opposing group on the first principal component axis. TChl-*a* and Si were correlated mostly with PC2. Overall, event-driven Mn variability was mainly independent of the other variables and the first two PCs.

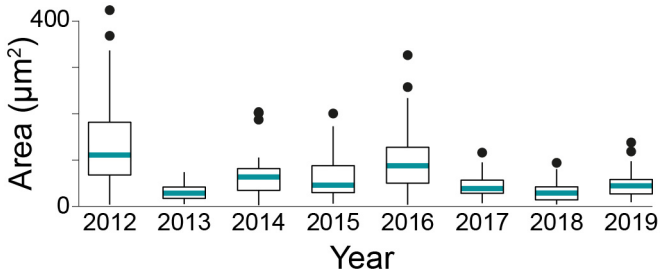

Fig. 5. Boxplots of the spring calcite layer grain size (planar area).

4. Discussion

4.1. Preservation of environmental signals in the sediment record

Lake Żabińskie's thermic structure and mixing regime exhibit a strong relationship with the atmosphere; especially surface waters react quickly and mirror air temperature changes (Fig. 6). Additionally, surface water temperature changes coincide to some extent with periods of increased windiness. Generally, heat fluxes vary the most at the water surface, while deeper strata exhibit more stability (Fig. 2a). Typical for temperate lakes, spring mixing in Lake Żabińskie starts immediately after the ice-cover break-up. Years characterized by a severe winter and long-lasting ice-cover typically result in short spring mixis followed by the rapid development of summer stratification. A short spring mixis is generally insufficient to oxygenate the hypolimnion, which results in prolonged anoxia. This is most clearly visible in 2013 and 2018, when the homothermic spring phases lasted for 3 and 2 days, respectively (Figs. 2a, 6). Overall, these years are characterized by lower MAR, whereas years with mild winters and prolonged spring mixing favor higher primary production and more intense calcite precipitation during spring, which results in higher MAR. Calcite precipitation dynamics are controlled mostly by water temperature and pH, as well as phytoplankton activity which is, in turn, limited by N and P concentrations (Stabel, 1986). In Lake Żabińskie, high nutrient concentrations in the surface waters after the ice-out can further rise due to lake turnover and internal loading from the deeper water strata. Then, with the rapid air temperature rise and subsequent warming of the epilimnion, intensive algae blooms (Fig. 2d) lead to HCO_3^- depletion and $CaCO_3$ supersaturation (Bonk et al., 2015a). Spring temperature increases over the scale of days further limit CO_2 solubility, leading to a quick increase of water pH (Fig. 2c, d, S2c S2d). Finally, this leads to rapid calcite precipitation, as seen in a drop of Ca^{2+} concentrations and a peak in TIC deposition registered in the sediment trap (Fig. 3b). Moreover, additional calcite precipitation events occur 2–3 times per varve year, as evidenced by sediment trap and sediment core data (Figs. 3b, 6, S4, S5, S9).

A gradual temperature rise and a warm summer also lead to an elevated accumulation of organic matter in the second half of the year (Fig. 3b). Furthermore, after warm summers, surface water cools quickly. In contrast, cold summers result in a more gradual decrease of water temperatures due to larger thermal inertia (Piccolroaz et al., 2015). Higher wind speeds at the end of the year typically increased fall destratification and mixing duration (Fig. 6). Increased wind speed can lead to more intense resuspension and redeposition of sediments (sediment focusing) which, to some extent, can explain higher mass accumulation rates registered shortly before and after the fall turnover in the sediments (Fig. 3b; Czymzik et al., 2016; Apolinarska et al., 2020; Roeser et al., 2021). Finally, the development of reverse stratification precedes ice-cover and calm sedimentation conditions under ice-cover. Mass accumulation rates during winter are generally lowest (Fig. 3b).

Comparison of sediment trap data and sediment core data allows us to assess how effectively the environmental signal is recorded in the sedimentary archive. The most basic parameter is MAR, which can be precisely estimated both from sediment traps and varved sediment cores. On average, during the study period, values of total MAR for individual years deviated in both datasets by 21 %. However, direct comparison is not possible for the varve year 2012 because the sediment trap was installed too late to register the first calcite precipitation event. Data from other years suggest that spring (April–May) deposition constitutes up to 53 % of the total MAR for each year. Accounting for this loss, annual deposition in 2012 sediment trap data agrees with MAR from the sediment core (Fig. 6), and after the correction, the mean difference during the study period is between 14 % and 17 %. Also, higher MAR for the varve year 2019 calculated from the sediment core could be an effect of imprecise subsampling in the very topmost section of the core, i.e., including part of the spring 2020 calcite layer. The only difference, which is difficult to explain, was registered in 2013 when data from the sediment trap showed much lower MAR. Minor differences should be expected, as sediment trap data averaged over the varve year cannot perfectly match core sub-sampling.

A high-resolution, sub-seasonal comparison between the sediment trap and core is possible using biogeochemical data. Total inorganic carbon concentrations measured in the sediment trap samples and µXRF Ca record provide evidence that, despite different temporal resolutions, both records track the same processes, ultimately leading to the formation and preservation of distinct calcite laminae. TIC concentrations measured in the sediment trap material typically show two or more peaks each year (Fig. 3b), corresponding to the layers visible in the thin sections. However, due to the temporal resolution of sediment traps, $CaCO_3$ peaks are smoothed. A similar pattern is visible in the µXRF Ca record, while the higher measurement resolution better captures well-defined local maxima corresponding to discrete calcite layers visible in thin sections (Fig. 4). After deposition, calcite layers do not undergo significant transformation, and post-depositional processes do not change the initial signal recorded at the time of layer formation. However, it is important to note that TIC is not solely $CaCO_3$, as Mn-carbonates are also present in the sediments, at times constituting up to 15 % of annual mineral material (Table S1). Therefore, inorganic carbon concentrations are controlled by more than one mineral and can diverge from µXRF Ca record. Typically, a similar overlap is visible between the total sulfur concentrations measured in the sediment trap samples (Fig. 3b) and µXRF S recorded from the sediment core (Fig. 5). Although sulfur accumulation is associated with dark laminae lacking well-developed sedimentary structures, it can be attributed to the second half of the varve year.

To summarize, surface sediments record the same variability of processes as the sediment traps. This allows a close match between the datasets measured over different scales – temporal for observational data and depth for core data. Finally, close links between meteorological and limnological conditions and varve formation processes can be observed and described.

4.2. Varve composition as a proxy for meteorological conditions and lake mixing regime

Calcite lamination characteristics have been previously used to reconstruct overall lake ontogeny in response to environmental change (Bonk et al., 2021; Hernández-Almeida et al., 2017) but also more specific climate parameters, e.g., past precipitation variability (Czymzik et al., 2016). Despite factors such as sediment redeposition, seasonal changes in meteorological conditions generally play a dominant role in the formation of biochemical varves, as seen in other mid-latitude lakes (Apolinarska et al., 2020;

Fig. 6. Links between atmospheric conditions (temperature, wind), water column properties (temperature at 1 m depth, oxycline depth and mixing regime), modern sedimentation observations, and sediment record. Mixis (F) – fall mixis; Mixis (S) – spring mixis; Stratification (W) – winter stratification; Stratification (S) – summer stratification. The first bar in the sediment trap MAR plot shows the observed and corrected value for 2012 using average spring (April–May) MAR values between 2013 and 2019 to replace missing data. The position of diagnostic layers is based on the dates of sediment trap TIC peaks, meteorological data and holomixis events. µXRF data is stretched to fit the diagnostic layers. Dots mark the beginning of varve year.

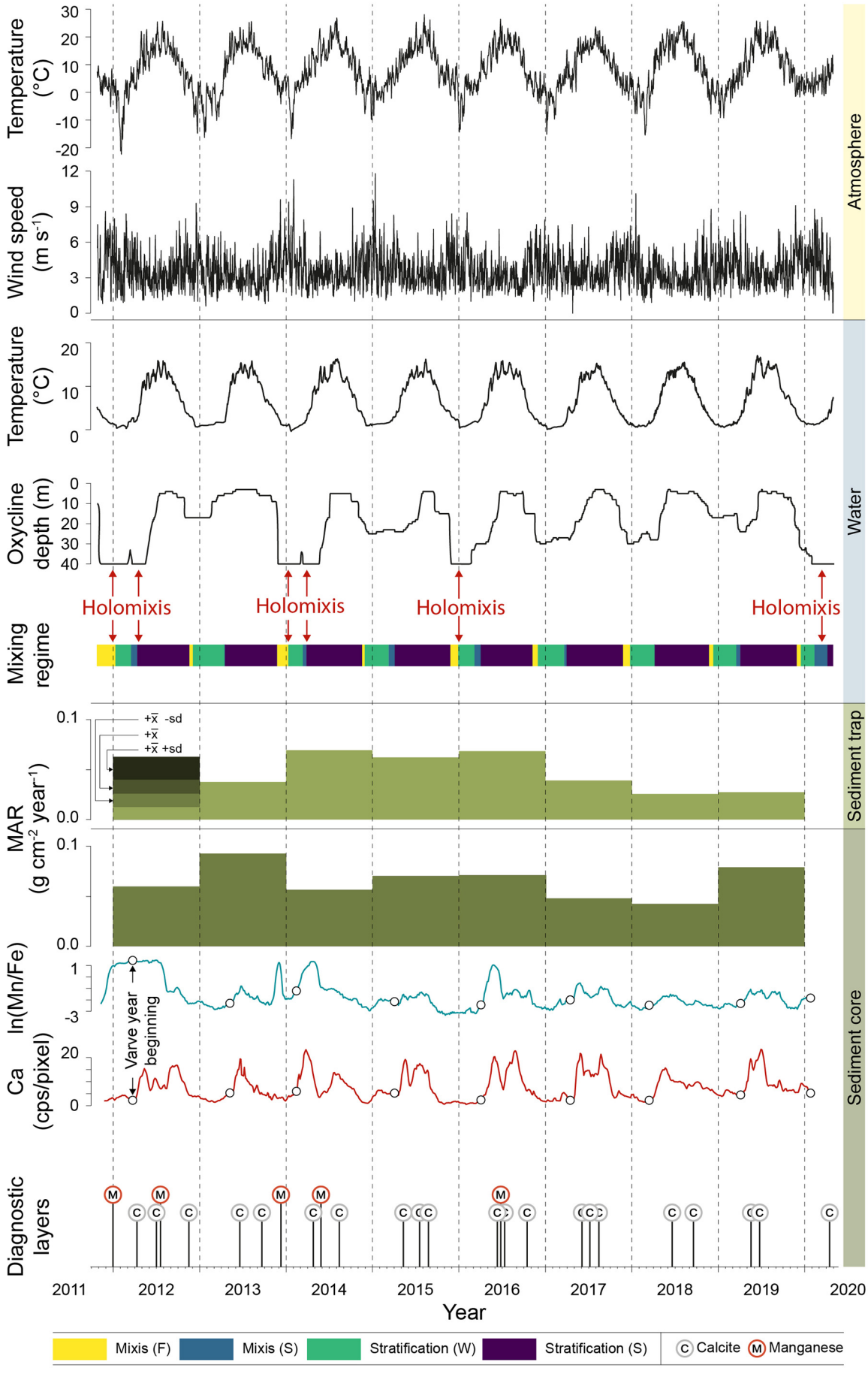
Temperature (°C)
Wind speed (m s-1)
Atmosphere
Temperature (°C)
Oxycline depth (m)
Holomixis
Holomixis
Holomixis
Holomixis
Mixing regime
Water
+x̄ -sd
+x̄
+x̄ +sd
MAR (g cm-2 year-1)
Sediment trap
ln(Mn/Fe)
Ca (cps/pixel)
Varve year beginning
Sediment core
Diagnostic layers
2011
2012
2013
2014
2015
2016
2017
2018
2019
2020
Year
Mixis (F)
Mixis (S)
Stratification (W)
Stratification (S)
Calcite
Manganese

Tylmann et al., 2012). Recently, Zander et al. (2021a) carried out a detailed investigation on the relationship between the Lake Żabińskie sediments and the meteorological conditions in the last ca. 60 years. Bulk geochemical data, especially total carbon (TC), show close relationships to the warm season (MAMJJA) air temperature ($r = 0.69, p < 0.05$) and spring (MAM) windspeeds ($r = -0.58, p < 0.05$). However, sediment micromorphology and sediment trap data can also reflect sub-seasonal changes in the atmosphere and lake (Roeser et al., 2021). Similarly, the complex microstructure of varves in Lake Żabińskie potentially also reflects specific weather phenomena.

The first calcite layer is always deposited immediately after the spring algae bloom (Bonk et al., 2015a; Żarczyński et al., 2018). Typically, the dynamics of $CaCO_3$ precipitation affect the grain size of calcite crystals (Fig. 5). Spring mixing intensity controls internal nutrient loadings. Elevated PO_4^{3-} concentrations in the epilimnion increase primary production and at the same time prevent rapid precipitation of small calcite grains (Lotter et al., 1997; Ohlendorf and Sturm, 2001). Long and intense spring mixing causes increased turbulence, numerous nucleation centers, and rapid growth of $CaCO_3$ and leads to a larger mean size of calcite grains (Lotter et al., 1997). During the last decade in Lake Żabińskie, this process was evident in 2012 and 2016 (Fig. 5). Precipitation of the second and third calcite laminae follows rapid cooling followed by warming of air and water and periods of increased wind speed lasting from days to weeks (Fig. 6). These changes exert control on the bicarbonate balance in the epilimnion and $CaCO_3$ saturation (Figs. 2c, S2c). Higher wind speeds cause shallow mixing events restricted to the first few meters of the water column. The Ca^{2+} pool depleted by $CaCO_3$ precipitation is briefly replenished by these shallow mixing events (Hernández-Almeida et al., 2015). These events also lead to decreased surface water temperatures, increased pH, and hinder photosynthesis, while increased turbulence allows diatoms to remain suspended (Bluszcz et al., 2008; Stabel, 1986). Subsequent algae blooms and epilimnion decalcification are driven by rising water temperature.

Furthermore, $CaCO_3$ is bound to abundant *Phacotus Lenticularis* lorica (Lenz, 2020; Roeser et al., 2021) found within the secondary calcite layers and in the summer sediment trap samples. High *Phacotus* abundances correspond to the short periods of increased windiness (Fig. S5) and rapid calcite precipitation (Figs. S4, S5). Because epilimnetic waters are depleted concerning Ca^{2+} and nutrients during the summer stratification, secondary calcite laminations are less developed and thinner than the spring layers (Figs. 4, S6). Years characterized by a late break-up of the ice-cover and no evident temperature shifts throughout the summer stratification are characterized by low and highly dispersed calcite precipitation, with no apparent separation between the calcite layers, as is seen in the years 2013 and 2018. Typical for low-P conditions and $CaCO_3$ supersaturation, sustained by high water temperature, these calcite layers are composed of smaller grains than those in the spring laminae (Lotter et al., 1997; Roeser et al., 2021). Additionally, (re)dissolution can influence the quantity of calcite deposited on the anoxic lake bed than its precipitation from the epilimnion (Dean, 1999), as evidenced by more irregular-shaped crystals deposited in years characterized by anoxic conditions. Overall, calcite precipitation in Lake Żabińskie is governed by rapid changes in the air and water temperature at the scale of weeks, and is further influenced by wind intensity controlling the mixing regime (Fig. 6).

It is challenging to track the timing and intensity of the lake water column mixing events with data from sediment cores. Abundances of redox-sensitive elements such as Mn and Fe are often regarded as proxies for changing oxygen conditions in the hypolimnion (Tribovillard et al., 2006). Previous studies suggest that the formation and preservation of Mn-bearing minerals in sediments is a complex problem with numerous plausible pathways for Mn burial (Davison et al., 1982). Changes in the O_2 availability (Dräger et al., 2017; Naeher et al., 2013) and pH (Bonk et al., 2021) are most often regarded as the primary controls of this process. Our observational data suggest a strong link between lake turnover, hypolimnion oxygenation, and Mn burial in the Lake Żabińskie sediments. Incidental Mn peaks are diagnostic for the holomixis events in Lake Żabińskie (Fig. 6, S2 and S8). During the observational period, every instance of holomixis produced a distinct Mn peak in the sediments, and there were no holomixis events that did not lead to elevated Mn concentrations in the sediments. Additionally, principal component analysis shows that Mn variability is mostly independent of the lithogenic proxies K and Ti (Fig. S7), suggesting redox-controlled Mn deposition (Zander et al., 2021b; Żarczyński et al., 2019). Bphe-*a* concentrations and S counts directly oppose Mn (Figs. 4, S7), further suggesting that oxygen availability drives Mn deposition in the sediments.

These findings align with results from several other seasonally anoxic lakes, such as Lake Stechlin, Germany (Scholtysik et al., 2020) and Baldeggersee, Switzerland (Schaller and Wehrli, 1997), where Mn-enriched layers are observed due to the process of geochemical focusing. This geochemical focusing results from repeated redox changes and the cycling of redox-sensitive species. During thermal stratification, Mn^{2+} is reductively dissolved and removed from sediments overlain by anoxic waters. When oxygen mixes with the Mn-rich hypolimnion, (oxy)hydroxide rains can occur, as observed in Elk Lake (Nuhfer et al., 1993); however, the majority of these (oxy)hydroxide particulates are (re)dissolved before burial in the deepest part of the lake. This leads to substantial enrichment of Mn^{2+} in the hypolimnion. During holomixis events, Mn-oxides are deposited at the deepest point, sometimes as thick crusts (Wirth et al., 2013). Subsequent stratification and reestablishment of anoxic conditions likely leads to the dissolution of a portion of the Mn-oxides formed during deep mixing, but conversion to Mn-carbonate, which is enabled by H_2S oxidation (Meister et al., 2009), leads to the preservation of Mn in anoxic sediments. In Lake Żabińskie, rhodochrosite constitutes up to 15 % of the mineral components in annual layers characterized by holomixis during the preceding fall or spring (2012 and 2014, Table S1). Distinct Mn-rich lamina visible in the μXRF maps (Fig. S8) suggests that Mn-carbonate formation is rapid in response to mixing events. Lake turnover can also induce Mn precipitation when the carbonate-rich surface waters mix with the Mn enriched bottom waters (Dean and Megard, 1993). We observe that spring holomixis leads to Mn enrichments that are intercalated within calcite laminae, whereas fall mixing typically leads to formation of Mn layers that clearly precede the onset of spring calcite precipitation. This observation shows the potential to reconstruct the frequency and timing of mixing events (fall versus spring) from the sedimentary record.

5. Conclusions

We investigated Lake Żabińskie in northeast Poland to explore the processes of biochemical varve formation and potential for climate signals preservation in these sediments. The combination of meteorological data, lake monitoring data, the composition of sediment trap samples, and sediment core analyses enabled us to identify influences of meteorological conditions on the sediment formation in this lake:

1. We see direct relationships between meteorological conditions, limnological processes, and modern sedimentation. Especially air temperature and wind speed directly affect physicochemical water parameters and primary production, which, together, govern the behavior of the inorganic carbon complex. Carbonate precipitation processes, geochemical focusing, and sedimentation of organic matter are the immediate effects of atmosphere-water interactions, yielding unique seasonal sediment structures and properties.
2. Variability in MAR and sediment composition observed in sediment trap samples is well reproduced in the sediment record. Therefore, good preservation of major environmental signals makes the sediment archive a reliable source of information for paleoenvironmental reconstructions.
3. Varves provide useful proxies for tracking meteorological and limnological processes in the past. In eutrophic lakes with biochemical varves, calcite laminae are the most characteristic feature of the sediment structure. In Lake Żabińskie, the grain size of the first (spring) calcite laminae is positively related to the intensity of spring mixing, while the occurrence of additional calcite laminae informs about colder and more windy periods during summer stratification. Furthermore, incidental

Mn peaks in sediments correspond perfectly with hypolimnetic oxygenation and holomixis events, suggesting that Mn is an excellent recorder of deep mixing events at this site. Holomixis events tend to occur during relatively long and cold springs or in fall/early winter due to the late formation of ice-cover on the lake.

Our study confirms that comprehensive observations of limnological parameters combined with high-resolution sediment analyses enable the recognition of a processing cascade leading to sediment formation and climate signal preservation. Observational data and novel high-resolution spectroscopic methods of sediment analysis show promise in tracking paleoweather phenomena using biochemical varved lake sediments. Further studies based on long-term observations of the atmosphere, hydrosphere, and lake sediments utilizing high-resolution data from the automated data loggers combined with ultra-high-resolution measurements of sediment fluxes might lead to even more accurate attribution of short duration events, e.g. heavy rainfall or increased wind speed, to sediment accumulation dynamics. Using already existing methods of non-destructive sediment analyses, it should also be possible to track the effects of these short-term events in micromorphology and geochemical variability of the sediment record.

CRediT authorship contribution statement

Maurycy Żarczyński: Conceptualization, Formal analysis, Investigation, Writing - original draft, Visualization. **Paul D. Zander**: Conceptualization, Investigation, Writing - review & editing, Visualization. **Wojciech Tylmann**: Conceptualization, Resources, Writing - review & editing, Project administration, Funding acquisition, Supervision, Resources. **Martin Grosjean**: Conceptualization, Resources, Writing - review & editing, Project administration, Funding acquisition.

Declaration of competing interest

The authors declare that they have no known competing financial interests or personal relationships that could have appeared to influence the work reported in this paper.

Acknowledgments

This research was funded by the National Science Centre grant 2015/18/E/ST10/00325 and Swiss National Science Foundation grant 200021_172586. We thank our colleagues who helped in the monitoring data collection: Paulina Głowacka, Kamil Nowiński, Dariusz Borowiak, Alicja Bonk and Agnieszka Szczerba. We thank Shauna-kay Rainford for help with μXRF geochemical mapping and Wolfgang Jan Zucha for help with pXRD analysis. We thank Anthony Chappaz and the anonymous reviewers for their thoughtful comments.

Appendix A. Supplementary data

Supplementary data to this article can be found online at https://doi.org/10.1016/j.scitotenv.2022.156787.

References

Amann, B., Lamoureux, S.F., Boreux, M.P., 2017. Winter temperature conditions (1670–2010) reconstructed from varved sediments, western Canadian High Arctic. Quat. Sci. Rev. 172, 1–14. https://doi.org/10.1016/j.quascirev.2017.07.013.

Apolinarska, K., Pleskot, K., Pełechata, A., Migdałek, M., Siepak, M., Pełechaty, M., 2020. The recent deposition of laminated sediments in highly eutrophic Lake Kierskie, western Poland: 1 year pilot study of limnological monitoring and sediment traps. J. Paleolimnol. https://doi.org/10.1007/s10933-020-00116-2.

Bergerhoff, G., Brown, I.D., Allen, F., 1987. Crystallographic Databases. International Union of Crystallography, Chester.

Bluszcz, P., Kirilova, E., Lotter, A.F., Ohlendorf, C., Zolitschka, B., 2008. Global radiation and onset of stratification as forcing factors of seasonal carbonate and organic matter flux dynamics in a hypertrophic hardwater lake (Sacrower see, northeastern Germany). Aquat. Geochem. 14, 73–98. https://doi.org/10.1007/s10498-008-9026-3.

Bonk, A., Tylmann, W., Amann, B., Enters, D., Grosjean, M., 2015a. Modern limnology, sediment accumulation and varve formation processes in Lake Żabińskie, northeastern Poland: comprehensive process studies as a key to understand the sediment record. J. Limnol. 74, 358–370. https://doi.org/10.4081/jlimnol.2014.1117.

Bonk, A., Tylmann, W., Goslar, T., Wacnik, A., Grosjean, M., 2015b. Comparing varve counting and 14C-ams chronologies in the sediments of Lake Żabińskie, northeastern Poland: implications for accurate 14C dating of lake sediments. Geochronometria 42. https://doi.org/10.1515/geochr-2015-0019.

Bonk, A., Müller, D., Ramisch, A., Kramkowski, M.A., Noryśkiewicz, A.M., Sekudewicz, I., Gąsiorowski, M., Luberda-Durnaś, K., Słowiński, M., Schwab, M., Tjallingii, R., Brauer, A., Błaszkiewicz, M., 2021. Varve microfacies and chronology from a new sediment record of Lake Gościąż (Poland). Quat. Sci. Rev. 251, 106715. https://doi.org/10.1016/j.quascirev.2020.106715.

Brauer, A., Casanova, J., 2001. Chronology and depositional processes of the laminated sediment record from Lac d'Annecy, French Alps. J. Paleolimnol. 25, 163–177.

Butz, C., Grosjean, M., Fischer, D., Wunderle, S., Tylmann, W., Rein, B., 2015. Hyperspectral imaging spectroscopy: a promising method for the biogeochemical analysis of lake sediments. J. Appl. Remote. Sens. 9, 096031. https://doi.org/10.1117/1.JRS.9.096031.

Butz, C., Grosjean, M., Poraj-Górska, A., Enters, D., Tylmann, W., 2016. Sedimentary Bacteriopheophytin a as an indicator of meromixis in varved Lake sediments of Lake Jaczno, north-east Poland, CE 1891–2010. Glob. Planet. Chang. 144, 109–118. https://doi.org/10.1016/j.gloplacha.2016.07.012.

Butz, C., Grosjean, M., Goslar, T., Tylmann, W., 2017. Hyperspectral imaging of sedimentary bacterial pigments: a 1700-year history of meromixis from varved Lake Jaczno, Northeast Poland. J. Paleolimnol. 58, 57–72. https://doi.org/10.1007/s10933-017-9955-1.

Cohen, A.S., 2003. Paleolimnology: The History And Evolution of Lake Systems. Oxford University Press, Oxford, New York.

Croudace, I.W., Löwemark, L., Tjallingii, R., Zolitschka, B., 2019. High resolution XRF core scanners: a key tool for the environmental and palaeoclimate sciences. Quat. Int. 514, 1–4. https://doi.org/10.1016/j.quaint.2019.05.038.

Czernecki, B., Głogowski, A., Nowosad, J., 2020. Climate: an R package to access free in-situ meteorological and hydrological datasets for environmental assessment. Sustainability 12, 394. https://doi.org/10.3390/su12010394.

Czymzik, M., Dreibrodt, S., Feeser, I., Adolphi, F., Brauer, A., 2016. Mid-Holocene humid periods reconstructed from calcite varves of the Lake Woserin sediment record (north-eastern Germany). The Holocene 26, 935–946. https://doi.org/10.1177/0959683615622549.

Davison, W., Woof, C., Rigg, E., 1982. The dynamics of iron and manganese in a seasonally anoxic lake; direct measurement of fluxes using sediment traps. Limnol. Oceanogr. 27, 987–1003. https://doi.org/10.4319/lo.1982.27.6.0987.

Dean, W.E., 1999. The carbon cycle and biogeochemical dynamics in lake sediments. J. Paleolimnol. 21, 375–393.

Dean, W.E., Megard, R.O., 1993. Environment of deposition of CaCO3 in Elk Lake, Minnesota. Geological Society of America Special Papers. Geological Society of America, pp. 97–114. https://doi.org/10.1130/SPE276-p97.

Dräger, N., Theuerkauf, M., Szeroczyńska, K., Wulf, S., Tjallingii, R., Plessen, B., Kienel, U., Brauer, A., 2017. Varve microfacies and varve preservation record of climate change and human impact for the last 6000 years at Lake Tiefer See (NE Germany). The Holocene 27, 450–464. https://doi.org/10.1177/0959683616660173.

Ersts, P.J., 2020. DotDotGoose. American Museum of Natural History, Center for Biodiversity and Conservation.

Evans, R.D., 1994. Empirical evidence of the importance of sediment resuspension in lakes. Hydrobiologia 284, 5–12. https://doi.org/10.1007/BF00005727.

Fojutowski, M., Gierszewski, P., Brykała, D., Bonk, A., Błaszkiewicz, M., Kramkowski, M., 2021. Spatio-temporal differences of sediment accumulation rate in the Lake Gościąż (Central Poland) as a response of meteorological conditions and lake basin morphometry. Cuad.Investig.Geogr. https://doi.org/10.18172/cig.4724.

Francus, P., Bradley, R.S., Abbott, M.B., Patridge, W., Keimig, F., 2002. Paleoclimate studies of minerogenic sediments using annually resolved textural parameters: paleoclimate studies of minerogenic sediments. Geophys. Res. Lett. 29, 59-1–59-4. https://doi.org/10.1029/2002GL015082.

Hernández-Almeida, I., Grosjean, M., Tylmann, W., Bonk, A., 2015. Chrysophyte cyst-inferred variability of warm season lake water chemistry and climate in northern Poland: training set and downcore reconstruction. J. Paleolimnol. 53, 123–138. https://doi.org/10.1007/s10933-014-9812-4.

Hernández-Almeida, I., Grosjean, M., Gómez-Navarro, J.J., Larocque-Tobler, I., Bonk, A., Enters, D., Ustrzycka, A., Piotrowska, N., Przybylak, R., Wacnik, A., Witak, M., Tylmann, W., 2017. Resilience, rapid transitions and regime shifts: fingerprinting the responses of Lake Żabińskie (NE Poland) to climate variability and human disturbance since AD 1000. The Holocene 27, 258–270. https://doi.org/10.1177/0959683616658529.

Hutorowicz, H., Grabowska, K., Nowicka, A., 1996. Charakterystyka warunków klimatycznych Pojezierza Mazurskiego. Zeszyty Problemowe Postępów Nauk Rolniczych 431, 21–29.

Idso, S.B., 1973. On the concept of lake stability1. Limnol. Oceanogr. 18, 681–683. https://doi.org/10.4319/lo.1973.18.4.0681.

Kienel, U., Dulski, P., Ott, F., Lorenz, S., Brauer, A., 2013. Recently induced anoxia leading to the preservation of seasonal laminae in two NE-German lakes. J. Paleolimnol. 50, 535–544. https://doi.org/10.1007/s10933-013-9745-3.

Lamoureux, S., 2000. Five centuries of interannual sediment yield and rainfall-induced erosion in the Canadian High Arctic recorded in lacustrine varves. Water Resour. Res. 36, 309–318. https://doi.org/10.1029/1999WR900271.

Lenz, S., 2020. Contribution of the calcifying green alga Phacotus lenticularis to lake carbonate sequestration.

Lorenc, H., 2005. In: Lorenc, H. (Ed.), Atlas klimatu Polski [Climatic Atlas of Poland]. Instytut Meteorologii i Gospodarki Wodnej, Warszawa.

Lotter, A.F., Sturm, M., Teranes, J.L., Wehrli, B., 1997. Varve formation since 1885 and high-resolution varve analyses in hypertrophic Baldeggersee (Switzerland). Aquat.Sci. 59, 22. https://doi.org/10.1007/BF02522361.

Marks, L., Dzierżek, J., Janiszewski, R., Kaczorowski, J., Lindner, L., Majecka, A., Makos, M., Szymanek, M., Tołoczko-Pasek, A., Woronko, B., 2016. Quaternary stratigraphy and palaeogeography of Poland. Acta Geol. Pol. 66, 410–434. https://doi.org/10.1515/agp-2016-0018.

Meister, P., Bernasconi, S.M., Aiello, I.W., Vasconcelos, C., Mckenzie, J.A., 2009. Depth and controls of Ca-rhodochrosite precipitation in bioturbated sediments of the Eastern Equatorial Pacific, ODP Leg 201, Site 1226 and DSDP Leg 68, Site 503. Sedimentology 56, 1552–1568. https://doi.org/10.1111/j.1365-3091.2008.01046.x.

Naeher, S., Gilli, A., North, R.P., Hamann, Y., Schubert, C.J., 2013. Tracing bottom water oxygenation with sedimentary Mn/Fe ratios in Lake Zurich, Switzerland. Chem. Geol. 352, 125–133. https://doi.org/10.1016/j.chemgeo.2013.06.006.

Neukom, R., Steiger, N., Gómez-Navarro, J.J., Wang, J., Werner, J.P., 2019. No evidence for globally coherent warm and cold periods over the preindustrial common era. Nature 571, 550–554. https://doi.org/10.1038/s41586-019-1401-2.

Nuhfer, E.B., Anderson, R.Y., Bradbury, J.P., Dean, W.E., 1993. Modern sedimentation in Elk Lake, Clearwater County, Minnesota. Geological Society of America Special Papers. Geological Society of America, pp. 75–96. https://doi.org/10.1130/SPE276-p75.

Nürnberg, G.K., 1995. The anoxic factor, a quantitative measure of anoxia and fish species richness in Central Ontario Lakes. Trans. Am. Fish. Soc. 124, 677–686. https://doi.org/10.1577/1548-8659(1995)124<0677:TAFAQM>2.3.CO;2.

Ohlendorf, C., Sturm, M., 2001. Precipitation and dissolution of calcite in a swiss high Alpine lake. Arct. Antarct. Alp. Res. 33, 410–417. https://doi.org/10.1080/15230430.2001.12003449.

Ojala, A.E.K., Francus, P., Zolitschka, B., Besonen, M., Lamoureux, S.F., 2012. Characteristics of sedimentary varve chronologies – a review. Quat. Sci. Rev. 43, 45–60. https://doi.org/10.1016/j.quascirev.2012.04.006.

Ojala, A.E.K., Kosonen, E., Weckström, J., Korkonen, S., Korhola, A., 2013. Seasonal formation of clastic-biogenic varves: the potential for palaeoenvironmental interpretations. GFF 135, 237–247. https://doi.org/10.1080/11035897.2013.801925.

Piccolroaz, S., Toffolon, M., Majone, B., 2015. The role of stratification on lakes' thermal response: the case of Lake Superior. Water Resour. Res. 51, 7878–7894. https://doi.org/10.1002/2014WR016555.

Poraj-Górska, A.I., Żarczyński, M.J., Ahrens, A., Enters, D., Weisbrodt, D., Tylmann, W., 2017. Impact of historical land use changes on lacustrine sedimentation recorded in varved sediments of Lake Jaczno, northeastern Poland. Catena 153, 182–193. https://doi.org/10.1016/j.catena.2017.02.007.

R Core Team, 2022. R: A Language And Environment for Statistical Computing. R Foundation for Statistical Computing, Vienna, Austria.

Roeser, P., Dräger, N., Brykała, D., Ott, F., Pinkerneil, S., Gierszewski, P., Lindemann, C., Plessen, B., Brademann, B., Kaszubski, M., Fojutowski, M., Schwab, M.J., Słowiński, M., Błaszkiewicz, M., Brauer, A., 2021. Advances in understanding calcite varve formation: new insights from a dual lake monitoring approach in the southern Baltic lowlands. Boreas 50, 419–440. https://doi.org/10.1111/bor.12506.

Schaller, T., Wehrli, B., 1997. Geochemical-focusing of manganese in lake sediments - an indicator of deep-water oxygen conditions. Aquat. Geochem. 2, 359–378. https://doi.org/10.1007/BF00115977.

Scholtysik, G., Dellwig, O., Roeser, P., Arz, H.W., Casper, P., Herzog, C., Goldhammer, T., Hupfer, M., 2020. Geochemical focusing and sequestration of manganese during eutrophication of Lake Stechlin (NE Germany). Biogeochemistry 151, 313–334. https://doi.org/10.1007/s10533-020-00729-9.

Sinninghe Damsté, J.S., Schouten, S., 2006. Biological markers for anoxia in the photic zone of the water column. In: Volkman, J.K. (Ed.), Marine Organic Matter: Biomarkers, Isotopes And DNA, the Handbook of Environmental Chemistry. Springer, Berlin, Heidelberg, pp. 127–163. https://doi.org/10.1007/698_2_005.

Stabel, H.-H., 1986. Calcite precipitation in Lake Constance: chemical equilibrium, sedimentation, and nucleation by algae. Limnol. Oceanogr. 31, 1081–1094. https://doi.org/10.4319/lo.1986.31.5.1081.

Szumański, A., 2000. Objaśnienia do Szczegółowej Mapy Geologicznej Polski, Arkusz Giżycko (104) (Explanation to the Detailed Geological Map of Poland, Sheet Giżycko (104)). Państwowy Instytut Geologiczny, Warszawa.

Tribovillard, N., Algeo, T.J., Lyons, T., Riboulleau, A., 2006. Trace metals as paleoredox and paleoproductivity proxies: an update. Chem. Geol. 232, 12–32. https://doi.org/10.1016/j.chemgeo.2006.02.012.

Tylmann, W., Szpakowska, K., Ohlendorf, C., Woszczyk, M., Zolitschka, B., 2012. Conditions for deposition of annually laminated sediments in small meromictic lakes: a case study of Lake Suminko (northern Poland). J. Paleolimnol. 47, 55–70. https://doi.org/10.1007/s10933-011-9548-3.

Tylmann, W., Zolitschka, B., Enters, D., Ohlendorf, C., 2013. Laminated lake sediments in northeast Poland: distribution, preconditions for formation and potential for paleoenvironmental investigation. J. Paleolimnol. 50, 487–503. https://doi.org/10.1007/s10933-013-9741-7.

Wacnik, A., Tylmann, W., Bonk, A., Goslar, T., Enters, D., Meyer-Jacob, C., Grosjean, M., 2016. Determining the responses of vegetation to natural processes and human impacts in north-eastern Poland during the last millennium: combined pollen, geochemical and historical data. Veget. Hist. Archaeobot. 25, 479–498. https://doi.org/10.1007/s00334-016-0565-z.

Wickham, H., Averick, M., Bryan, J., Chang, W., McGowan, L., François, R., Grolemund, G., Hayes, A., Henry, L., Hester, J., Kuhn, M., Pedersen, T., Miller, E., Bache, S., Müller, K., Ooms, J., Robinson, D., Seidel, D., Spinu, V., Takahashi, K., Vaughan, D., Wilke, C., Woo, K., Yutani, H., 2019. Welcome to the Tidyverse. JOSS 4, 1686. https://doi.org/10.21105/joss.01686.

Winslow, L., Read, J., Woolway, R., Brentrup, J., Leach, T., Zwart, J., Albers, S., Collinge, D., 2019. rLakeAnalyzer: Lake Physics Tools.

Wirth, S.B., Gilli, A., Niemann, H., Dahl, T.W., Ravasi, D., Sax, N., Hamann, Y., Peduzzi, R., Peduzzi, S., Tonolla, M., Lehmann, M.F., Anselmetti, F.S., 2013. Combining sedimentological, trace metal (Mn, Mo) and molecular evidence for reconstructing past water-column redox conditions: the example of meromictic Lake Cadagno (Swiss Alps). Geochim. Cosmochim. Acta 120, 220–238. https://doi.org/10.1016/j.gca.2013.06.017.

Zander, P.D., Żarczyński, M., Tylmann, W., Rainford, S., Grosjean, M., 2021a. Seasonal climate signals preserved in biochemical varves: insights from novel high-resolution sediment scanning techniques. Clim. Past 17, 2055–2071. https://doi.org/10.5194/cp-17-2055-2021.

Zander, P.D., Żarczyński, M., Vogel, H., Tylmann, W., Wacnik, A., Sanchini, A., Grosjean, M., 2021b. A high-resolution record of Holocene primary productivity and water-column mixing from the varved sediments of Lake Żabińskie, Poland. Sci. Total Environ. 755, 143713. https://doi.org/10.1016/j.scitotenv.2020.143713.

Żarczyński, M., Tylmann, W., Goslar, T., 2018. Multiple varve chronologies for the last 2000 years from the sediments of Lake Żabińskie (northeastern Poland) – comparison of strategies for varve counting and uncertainty estimations. Quat. Geochronol. 47, 107–119. https://doi.org/10.1016/j.quageo.2018.06.001.

Żarczyński, M., Wacnik, A., Tylmann, W., 2019. Tracing lake mixing and oxygenation regime using the Fe/Mn ratio in varved sediments: 2000 year-long record of human-induced changes from Lake Żabińskie (NE Poland). Sci. Total Environ. 657, 585–596. https://doi.org/10.1016/j.scitotenv.2018.12.078.

Zolitschka, B., Francus, P., Ojala, A.E.K., Schimmelmann, A., 2015. Varves in lake sediments – a review. Quat. Sci. Rev. 117, 1–41. https://doi.org/10.1016/j.quascirev.2015.03.019.